Biodistribution of ^{211}At labeled HER-2 binding affibody molecules in mice

ANN-CHARLOTT STEFFEN[1], YLVA ALMQVIST[2], MING-KUAN CHYAN[3], HANS LUNDQVIST[1], VLADIMIR TOLMACHEV[1], D. SCOTT WILBUR[3] and JÖRGEN CARLSSON[1]

[1]Unit of Biomedical Radiation Sciences, Department of Oncology; [2]Unit of Radiology, Department of Oncology, Radiology and Clinical Immunology, Rudbeck Laboratory, Uppsala University, SE-751 85 Uppsala, Sweden; [3]Department of Radiation Oncology, University of Washington, Box 359658, 325 Ninth Avenue, Seattle, WA 98104-2499, USA

Received October 16, 2006; Accepted November 29, 2006

Abstract. The size of affibody molecules makes them suitable as targeting agents for targeted radiotherapy with the α-emitter ^{211}At, since their biokinetic properties match the short physical half-live of ^{211}At. In this study, the potential for this approach was investigated *in vivo*. Two different HER-2 binding affibody molecules were radiolabeled with ^{211}At using both the linker PAB (*N*-succinimidyl-*para*-astatobenzoate) and a decaborate-based linker, and the biodistribution in tumor-bearing nude mice was investigated. The influence of L-lysine and Na-thiocyanate on the ^{211}At uptake in normal tissues was also studied. Based on the biokinetic information obtained, the absorbed dose was calculated for different organs. Compared with a previous biodistribution with ^{125}I, the ^{211}At biodistribution using the PAB linker showed higher uptake in lungs, stomach, thyroid and salivary glands, indicating release of free ^{211}At. When the decaborate-based linker was used, the uptake in those organs was decreased, but instead, high uptake in kidneys and liver was found. The uptake, when using the PAB linker, could be significantly reduced in some organs by the use of L-lysine and/or Na-thiocyanate. In conclusion, affibody molecules have suitable blood-kinetics for targeted radionuclide therapy with ^{211}At. However, the labeling chemistry affects the distribution in normal organs to a high degree and needs to be improved to allow clinical use.

Introduction

Targeted radionuclide therapy is a promising way of treating cancer, especially when disseminated tumor cells and micro-metastases are present. Various targeting agents, directed against a number of tumor-associated antigens, have been developed. However, the radionuclides used are mainly ß-emitters, such as ^{131}I and ^{90}Y, which deposit their energy over a long distance [0.8 mm for ^{131}I and 5.3 mm for ^{90}Y (1)]. To be therapeutically effective, ß-emitters are dependent on cross-fire irradiation, which might result in dose-limiting toxicity to non-target tissues, such as bone marrow. If small cell clusters or single cells are to be effectively treated, radionuclides that deposit their energy within one or a few cell diameters, such as α-emitters, are required (1). The problems with α-emitters are that they are quite short-lived, and not commercially available (2). The most commonly used α-emitters for radionuclide therapy are ^{212}Bi, ^{213}Bi and ^{211}At. Of those, ^{211}At has the longest physical half-life, 7.2 h compared with 61 and 46 min, respectively for the Bi isotopes. Such short physical half-lives result in most decays occurring in the blood stream, before reaching the tumor. Therefore, it is important that the targeting agent finds its target fast. Peptides and small proteins, which have fast pharmacokinetics, are thus preferable for therapy with short-lived α-emitters.

We recently developed and evaluated a new type of targeting agent, a tumor targeting affibody molecule (3,4). The affibody molecules investigated, $Z_{HER2:4}$ and its bivalent version $(Z_{HER2:4})_2$, are directed against the membrane protein HER-2 (K_D = 50 and 3 nM, respectively), which is over-expressed in many breast and ovarian carcinomas, but appear to a much lower extent in normal adult tissue (5,6). The small size (7 kDa for the monovalent-, and 15 kDa for the bivalent affibody molecule) and high stability of the protein make it an interesting targeting agent for radionuclide therapy. The affibody molecule $(Z_{HER2:4})_2$ can be radiolabeled with both ^{125}I and ^{211}At using the precursor *N*-succinimidyl-*para*-(trimethylstannyl) benzoate, resulting in [^{125}I]PIB-$(Z_{HER2:4})_2$ and [^{211}At]PAB-$(Z_{HER2:4})_2$ (PAB = *N*-succinimidyl-*para*-astatobenzoate and PIB = *N*-succinimidyl-*para*-iodobenzoate) respectively. From previous experiments we know that the radioiodinated form resulted in a tumor-to-blood ratio of ~10 at 8-h post injection. The plasma half-life in the elimination phase was ~45 min (7). This time pattern should suite the physical half-life of ^{211}At (7.2 h).

Correspondence to: Dr Jörgen Carlsson, Unit of Biomedical Radiation Sciences, Department of Oncology, Radiology and Clinical Immunology, Rudbeck Laboratory, Uppsala University, SE-751 85 Uppsala, Sweden
E-mail: jorgen.carlsson@bms.uu.se

Key words: affibody, HER-2, ^{211}At, radionuclide therapy

Affinity maturation of the original HER-2 binding affibody molecule $Z_{HER2:4}$ was recently described (8). The affinity maturated affibody molecule, $Z_{HER2:342}$, shows a remarkably high affinity (K_D = 22 pM) for HER-2 and its non-radioactive form has stronger growth inhibiting properties compared with the previously studied affibody molecules (9).

In this study, two different HER-2 binding affibody molecules were labeled with ^{211}At and investigated *in vivo*. The therapeutic potential is discussed.

Materials and methods

Preparation of the B10 maleimide. Preparation of the decaborate-based linker molecule for site-specific thiol-coupled radiolabeling is described schematically in Fig. 1. $(Et_3NH)B_{10}H_9$-CO (1) (10) was coupled to trioxadimine (2). The resulting $(Et_3NH)B_{10}H_9$-CO-trioxadiamine (3) was then conjugated to NHS-3-Maleimido-propionate (Quanta Bio-Design, Powell, OH, USA) (4). The final product, the decaborate linker (5), was confirmed using NMR spectroscopy and mass spectrometry.

Radiolabeling. The ^{211}At was produced at Rigshospitalet, Copenhagen, Denmark, as described by Persson *et al* (11) and the astatine was separated from the target using dry distillation at our laboratory. The astatine was eluted in chloroform, which was evaporated under a gentle flow of argon gas. The ^{211}At was then dissolved in 10 μl acetic acid (0.1% in water) immediately before labeling.

PAB (*N*-succinimidyl-*para*-astatobenzoate) labeling was achieved using the precursor *N*-succinimidyl-*para*-(trimethylstannyl) benzoate, prepared according to Koziorowski *et al* (12). Immediately before labeling, it was dissolved in 5% acetic acid in methanol to a concentration of 1 mg/ml and 5 μl was added to a vial containing ^{211}At dissolved in 0.1% acetic acid. Addition of 10 μl chloramine-T (4 mg/ml in water; Sigma, St. Louis, MO, USA) started the reaction. After 5 min of constant shaking, the reaction was terminated by addition of 10 μl sodium meta-bisulphite (8 mg/ml in water; Aldrich, Steinheim, Germany). The astatinated linker molecule was then coupled to 60 μg of $Z_{HER2:342}$-cys or $(Z_{HER2:4})_2$ (2.4 mg/ml or 1.2 mg/ml in phosphate buffered saline (PBS), Affibody AB, Bromma, Sweden) by addition of 100 μl 0.07 M borate buffer (pH 9.4) followed by 45 min continuous shaking in room temperature. The astatinated affibody molecules, [^{211}At]PAB-$Z_{HER2:342}$-cys and [^{211}At]PAB-$(Z_{HER2:4})_2$, were then separated from free ^{211}At using gel filtration on a NAP-5 column (Amersham Biosciences, Uppsala, Sweden) equilibrated in PBS. The specific activities obtained varied between 0.3-3 MBq/μg.

The decaborate-based linker molecule (number 5 in Fig. 1), [13'-(N'-[3''-(maleimido)propionylamino]-4',7',10'-trioxatridecaneamino)-nonahydro-*closo*-decaborate carboxylic acid triethylammonium salt], was dissolved in dimethyl formamide to a concentration of 10 mg/ml and 3 μl was added to a vial containing ^{211}At dissolved in 0.1% acetic acid. Radiolabeling of the linker molecule was then performed as described above. The ^{211}At is expected to be associated to the boron atom(s) after this procedure. The radiolabeled linker molecule was then site-specifically conjugated to 100 μg (molar linker-to-protein-ratio ~3:1) $Z_{HER2:342}$-cys by addition of 200 μl PBS with 1 mM EDTA, pH 6.5. After 40 min of constant shaking in room temperature, the astatinated affibody molecule, designated [^{211}At]B10-$Z_{HER2:342}$-cys, was separated from free ^{211}At on a NAP-5 column equilibrated with PBS. DTT-mediated reduction of the affibody molecule prior to the conjugation was shown to be unnecessary. A specific activity of 8 kBq/μg was obtained after the procedure.

Animals. Female BALB/c nu/nu mice (18-23 g, Møllegaard, Denmark) were used in the tumor model, whereas female NMRI mice (24-27 g, B&K Universal, Sollentuna, Sweden) were used in the normal model. Intravenous (i.v.) injections were made via the tail vein. At the end of the experiments, the mice were anesthetized with a mixture of Ketalar and Rumpun and euthanized by heart puncture. Organs of interest were collected, weighed, and the γ-component of the decay was measured in an automated gamma counter (1480 Wizard, Wallac, Finland). Injected dose was calculated as the radioactivity in the control syringes subtracted by the radioactivity left in the tail and in the syringe.

Biodistribution of [^{211}At]PAB-$(Z_{HER2:4})_2$. BALB/c mice were injected, subcutaneously (s.c.) in the right flank, with $1.7x10^7$ SKOV-3 cells in 100 μl McCoy's 5A culture medium, supplemented with 10% bovine serum albumin, 2 mM L-glutamine and PEST (100 IU/ml penicillin, 100 μg/ml streptomycin), all from Biochrom KG (Berlin, Germany). One month later, when the tumor weight was ~100 mg, the mice were randomized into groups of four. All mice were injected i.v. with 50 μl (250 ng, ~700 kBq) [^{211}At]PAB-$(Z_{HER2:4})_2$. Forty minutes before injection of [^{211}At]PAB-$(Z_{HER2:4})_2$, one group of mice (blocked) was injected with 100 μg unlabeled $(Z_{HER2:4})_2$ in PBS s.c. in the neck to block the specific uptake of the radiolabeled compound. After 1, 4, 7, 14 and 21 h respectively (after 7 h also the blocked group), mice were euthanized and dissected, as described above. Percent injected dose per gram tissue (%ID/g) was calculated for all organs. For the thyroid, a standard weight of 5 mg for a 20 g mouse was used for calculations.

Biodistribution of [^{211}At]B10-$Z_{HER2:342}$-cys. Four NMRI mice were injected i.v. with 100 μl (1.4 μg, 11 kBq) [^{211}At]B10-$Z_{HER2:342}$-cys. Four hours later, the animals were sacrificed, and the organs were collected and weighted. The radioactivity in the isolated tissues was measured and %ID/g was calculated, as described above. The HER-2 binding capacity of the astatinated affibody was also tested on SKOV-3 cells *in vitro*. SKOV-3 cells (~200 000) were seeded in 3-cm culture dishes and the following day, ~40 ng of the astatinated affibody per dish was added to 6 dishes. To 3 of the dishes, an excess (~2 μg per dish) of unlabeled $Z_{HER2:342}$ was added to block the specific uptake.

Prevention of deastatination and astatide uptake. Sixteen NMRI mice were injected i.v. with 100 μl (1 μg, ~280 kBq) [^{211}At]PAB-$(Z_{HER2:4})_2$. The mice were divided into four groups. One group served as a control, and received only the

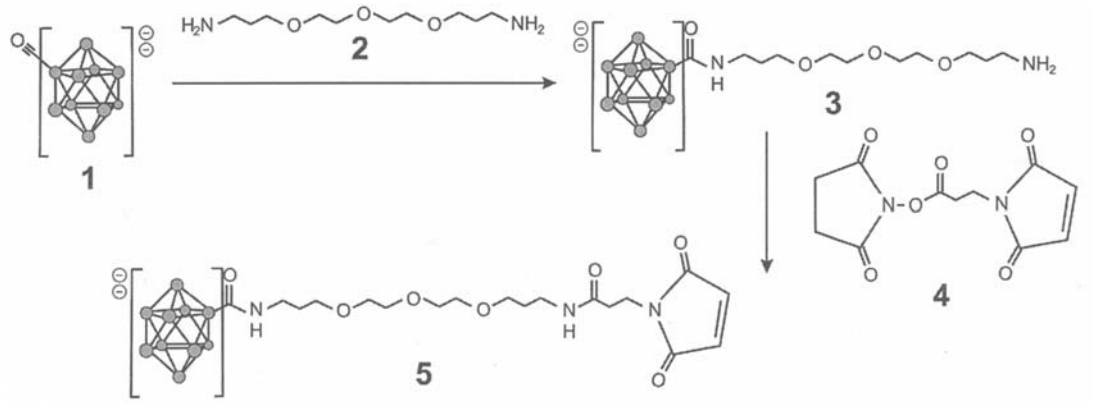

Figure 1. Preparation scheme for the B10 maleimide. White circles represent boron atoms in the decaborate(2-) cage.

radiolabeled compound. The next group received 2 mg L-lysine (Sigma) in PBS per gram body weight intraperitoneally (i.p.) 30 min before radioactive injection, as well as 1, 2 and 3 h after injection of [^{211}At]PAB-($Z_{HER2:4}$)$_2$. The third group received 97 μg Na-thiocyanate (Sigma-Aldrich, St. Louis, MO, USA) in PBS per gram body weight i.p. 24 and 1 h before the radioactive injection. The fourth group received both L-lysine and Na-thiocyanate as described above. Four hours after injection of [^{211}At]PAB-($Z_{HER2:4}$)$_2$ the mice were sacrificed and selected organs were collected, weighted and measured for radioactivity uptake.

Biodistribution of [^{211}At]PAB-$Z_{HER2:342}$-cys. Female BALB/c nu/nu mice were injected with 7.6x10^6 SKOV-3 cells s.c. in the right flank. The body weight and tumor size were carefully monitored for 40 days. Then, when the tumors had an average weight of 1 g, 100 μl [^{211}At]PAB-$Z_{HER2:342}$-cys (10 μg, ~160 kBq) in PBS was injected i.v. via the tail vein. Na-thiocyanate (150 μg/g body weight) was injected i.p. 24 h and 1 h before injection of radioactivity. L-lysine (2 mg/g body weight) was injected i.p. 30 min before, and 1, 2 and 3 h after injection of [^{211}At]PAB-$Z_{HER2:342}$-cys. Animals were placed in groups of four, and one group (blocked group) was injected with 1 mg unlabeled $Z_{HER2:342}$-cys s.c. in the neck region 35 min before radioactive injection, to block specific binding to the tumor. Mice were sacrificed 1, 2, 4, 8 and 16 h after injection of [^{211}At]PAB-$Z_{HER2:342}$-cys (after 4 h the blocked group was also taken). Organs and tissues of interest were collected and %ID/g was then calculated, as described above.

Statistical test. The Student's t-test was used to test the differences in tissue concentration of radioactivity, between different groups of animals. The level of significance was set at $p<0.05$.

Dosimetry calculations. In order to investigate the potential for a therapy study in mice, a dosimetry calculation was performed. The organ uptake values from the biodistribution of [^{211}At]PAB-$Z_{HER2:342}$-cys, non-corrected for physical half-life, were integrated over time to obtain the residence time per gram tissue for dosimetry calculations. Integration between time zero and 16 h was made by the trapezoid method. The two last time points were fitted to a single exponential function, which was used to estimate the residence time from 16 h to infinity. Except for the thyroid and stomach, the value of the extrapolated area was small in all organs compared to the area obtained between time zero and 16 h.

To obtain an error estimate of the absorbed dose, the uptake values were randomly generated from a normal distribution with the mean and standard deviations obtained from the biodistribution of [^{211}At]PAB-$Z_{HER2:342}$-cys. Using the experimental data, new uptake values were randomly generated with the assumption of a normal distribution. A set of 30 randomly produced uptake curves were then integrated as described above. This created a set of 30 randomly distributed residence time values. The relative standard deviation of the absorbed dose was taken to be the same as for this set of data.

In 58.2% of the ^{211}At decays, ^{211}Po ($T_{1/2}$ = 0.516 sec) is produced. Due to its short half-life, ^{211}Po is from a dosimetric point of view regarded to be in equilibrium with ^{211}At. The second branch of the ^{211}At-decay produces ^{207}Bi ($T_{1/2}$ = 34.4 a). Due to the long half-life and the low S-value for ^{207}Bi in relation to the ^{211}At/^{211}Po-decay, it does not significantly contribute to the absorbed dose and is neglected in the dosimetry calculations. S-values for ^{211}At and ^{211}Po were obtained from RADAR phantoms (Unit Density Spheres) (http://www.doseinfo-radar.com/RADARphan.html). These values were summarized, taken into account the decay abundance, to obtain a value of 1.09 mGy/(MBqxs) in one gram tissue. This value was multiplied with the organ residence values to obtain the organ absorbed dose. This simple dosimetry calculation is motivated by the fact that the main absorbed dose from the two radionuclides are given locally by the α-particles. Photons and other penetrating radiations are only contributing to a slight extent, which means that the cross-talk between different organs is negligible.

Results

Biodistribution of [^{211}At]PAB-($Z_{HER2:4}$)$_2$. As seen in Fig. 2, the biodistribution of [^{211}At]PAB-($Z_{HER2:4}$)$_2$ in tumor-bearing nude mice differed greatly from the biodistribution of [^{125}I]PIB-($Z_{HER2:4}$)$_2$ (PIB = *N*-succinimidyl-*para*-iodobenzoate), as previously reported (1). Markedly higher normal tissue

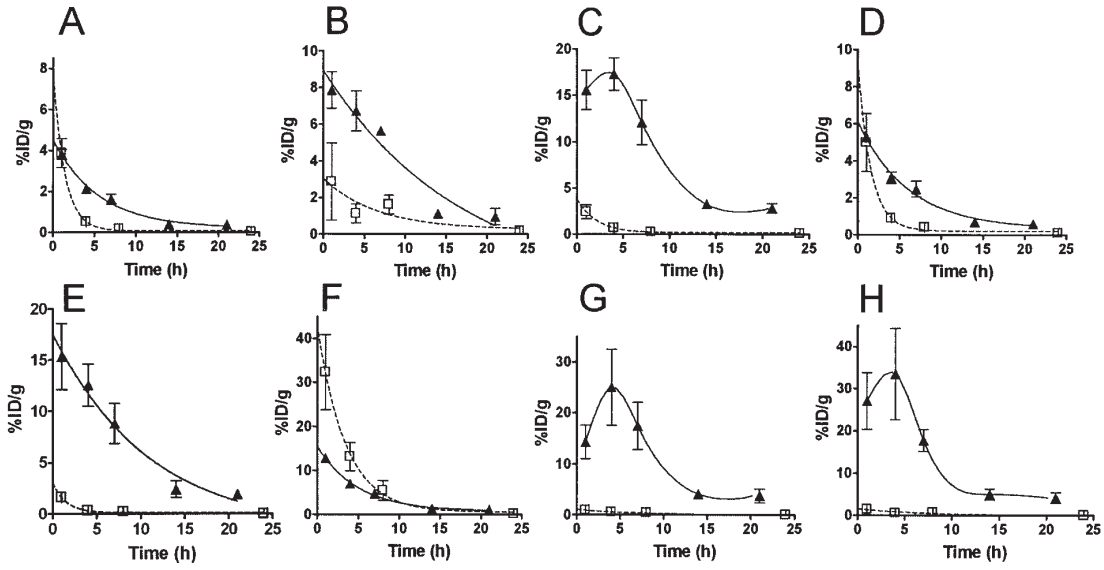

Figure 2. Comparison between the concentrations of [^{125}I]PIB-$(Z_{HER2:4})_2$ (1) (white squares) and [^{211}At]PAB-$(Z_{HER2:4})_2$ (black triangles) in selected tissues. The tissues in the graph are: (A) blood, (B) tumor, (C) lungs, (D) liver, (E) spleen, (F) kidneys, (G) stomach, and (H) salivary glands. Values are mean values obtained from four mice. Error bars are standard deviations.

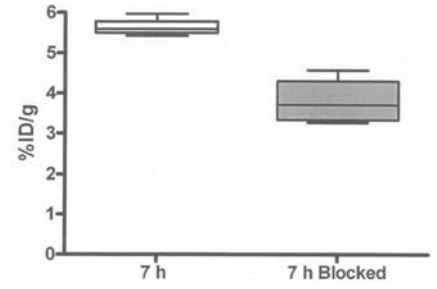

Figure 3. The specificity in tumor uptake 7 h after injection of [^{211}At]PAB-$(Z_{HER2:4})_2$. The blocked group received an excess of unlabeled $(Z_{HER2:4})_2$ to block the available binding sites. The box extends from the 25th percentile to the 75th percentile with a line at the median. The bars show the highest and lowest value. The tumor uptake was decreased (p=0.01) after injection of unlabeled $(Z_{HER2:4})_2$, indicating at least some specific uptake.

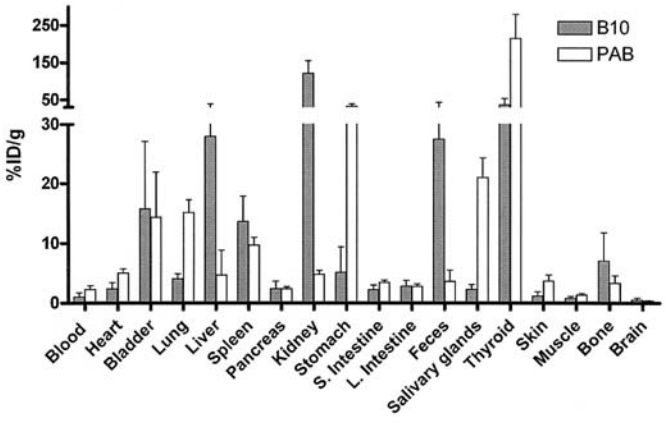

Figure 4. Biodistribution of [^{211}At]B10-$Z_{HER2:342}$-cys in NMRI mice 4-h post injection (gray bars) compared to [^{211}At]PAB-$(Z_{HER2:4})_2$ (white bars). Values are mean values obtained from four mice. Error bars are standard deviations. A standard thyroid weight of 5 mg/20 g mouse was used.

concentrations were seen in many organs, especially the lungs, spleen, stomach and salivary glands where significantly higher radionuclide concentrations were obtained with ^{211}At than in the earlier study with ^{125}I. In those organs, the uptake appeared to peak at the 4-h time-point, where 25-55 times more ^{211}At was found, compared with ^{125}I. As seen in Fig. 3, the amount of radioactivity in the tumor at 7-h post injection could be displaced by administration of unlabeled $(Z_{HER2:4})_2$, indicating receptor-specific tumor uptake.

Biodistribution of [^{211}At]B10-$Z_{HER2:342}$-cys. When the PAB linker molecule was exchanged for the decaborate-based B10, the high concentration of radioactivity in the lungs, stomach and salivary glands was markedly reduced, as seen in Fig. 4. However, the concentration in the spleen was not reduced, and the concentrations in liver and kidneys were markedly increased with the decaborate-based linker (6 times higher in the liver and 25 times higher in the kidneys). The thyroid uptake was somewhat reduced, but was still higher than the corresponding uptake of ^{125}I using the PIB linker (1). A binding test of [^{211}At]B10-$Z_{HER2:342}$-cys on SKOV-3 cells *in vitro*, according to a method described in Wikman *et al* (4), showed that the astatinated affibody bound to the cells in a specific manner (data not shown).

Prevention of deastatination and astatide uptake. As seen in Fig. 5, the addition of L-lysine reduced the concentration of radioactivity, after administration of [^{211}At]PAB-$(Z_{HER2:4})_2$, in stomach and salivary glands. However, the reduction was not significant in the salivary glands. Administration of sodium thiocyanate significantly reduced the uptake in stomach, salivary glands and thyroid and the combination of L-lysine and sodium thiocyanate reduced the uptake of ^{211}At even more.

Biodistribution of [^{211}At]PAB-$Z_{HER2:342}$-cys. Fig. 6 shows the biodistribution of [^{211}At]PAB-$Z_{HER2:342}$-cys in nude mice

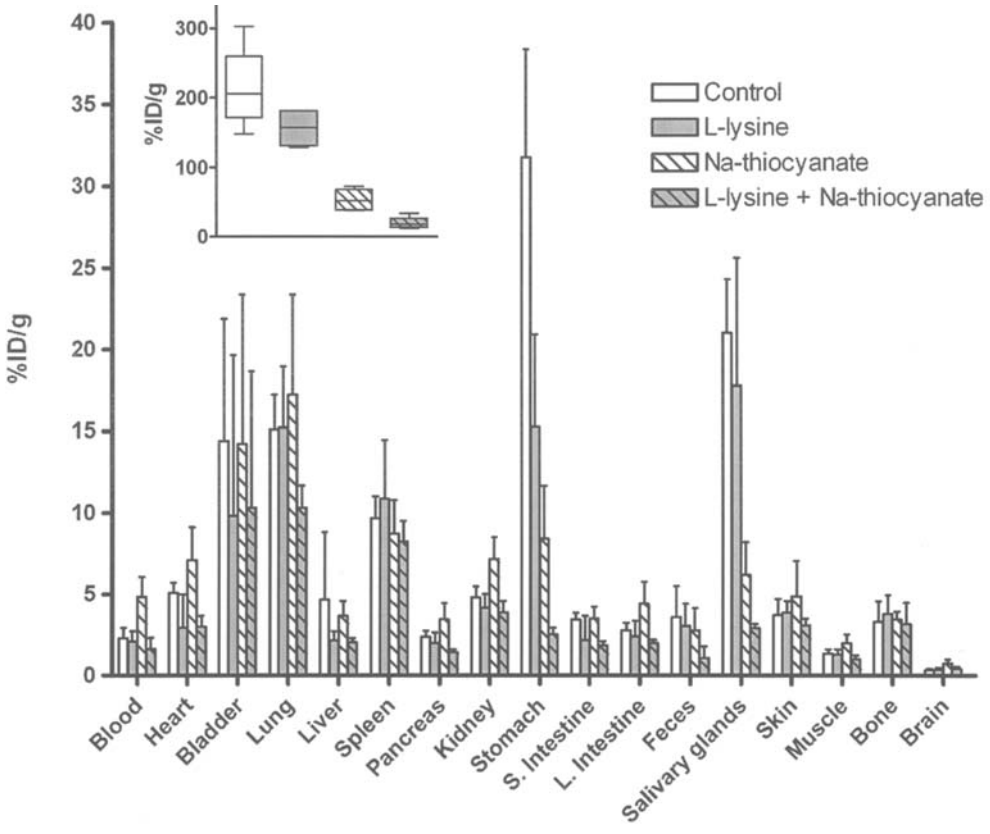

Figure 5. Biodistribution of [^{211}At]PAB-($Z_{HER2:4}$)$_2$ in normal mice 4 h after injection. White bars are controls, gray bars represent mice that received L-lysine, dashed bars represent mice that received Na-thiocyanate and gray dashed bars represent mice that received both of these substances. Values are mean values from four mice. Error bars are standard deviations. The inserted image shows the thyroid uptake (standard thyroid weight - 5 mg/20 g mouse) represented by a box that extends from the 25th percentile to the 75th percentile with a line at the median. The bars show the highest and lowest value.

carrying xenografted SKOV-3 tumors when degradation in the kidneys were blocked by administration of L-lysine 30 min before, and 1, 2, and 3 h after injection of the radiolabeled conjugate. The uptake of free ^{211}At was also blocked, by administration of Na-thiocyanate 24h and 1 h before injection of [^{211}At]PAB-$Z_{HER2:342}$-cys. As seen in Fig. 6, the concentration of radioactivity in the tumor was constantly ~7 %ID/g during the first 8 h, but decreased significantly after 16 h. The con-centration in lungs and spleen was high (~13 %ID/g) and almost constant during the first 8 h. The concentration in the thyroid increased with time, and reached 38 %ID/g at the 16-h time-point.

A Student's t-test comparing the tissue concentrations of radioactivity at the 4-h time-point between the group that received a large excess of unlabeled $Z_{HER2:342}$-cys to block-specific binding, and the group without such a block, revealed that the tumor concentration was significantly lower ($p<0.05$) in the blocked group, see inserted plot in Fig. 6. There was no significant difference in any other organ (data not shown).

Dosimetry calculations. The results from the simplified dosimetry calculations are summarized in Table I. The tumor received ~2 Gy/MBq, whereas lungs and spleen received ~4 Gy/MBq. The thyroid received the highest dose, ~17 Gy/MBq.

Discussion

The potential of the α-emitter ^{211}At in targeted radiotherapy for treatment of metastasized malignancies and residual disease has been widely claimed (13,14). A prerequisite for therapy with a short-lived nuclide like ^{211}At (physical half-life 7.2 h) is that the target is reached within a few hours and that the remaining radioactivity is quickly removed from the system. This makes intact antibodies unsuitable for therapy with ^{211}At, but smaller antibody fragments, like scFv can still be considered. In this study, the potential for ^{211}At therapy using affibody molecules was investigated for the first time.

Our results with the astatinated ($Z_{HER2:4}$)$_2$ shows that the biodistribution is markedly different from the previous biodistribution with the same compound labeled with ^{125}I. In most cases, the biodistribution of a protein radiolabeled with ^{125}I and ^{211}At are quite similar (11,15,16), but there have been previous reported exceptions (17,18), especially when smaller molecules, such as antibody fragments have been used. The results from these studies, with high uptake in stomach, lungs and spleen, indicate that free ^{211}At is released *in vivo*. The high level of radioactivity in the tumor in the ^{211}At case is probably a result of higher blood levels, compared to the ^{125}I case. The tumor uptake can partly be explained by unspecific localization of ^{211}At, since only ~1/3 of the radioactivity in the tumor could be displaced by administration of unlabeled ($Z_{HER2:4}$)$_2$ (Fig. 3).

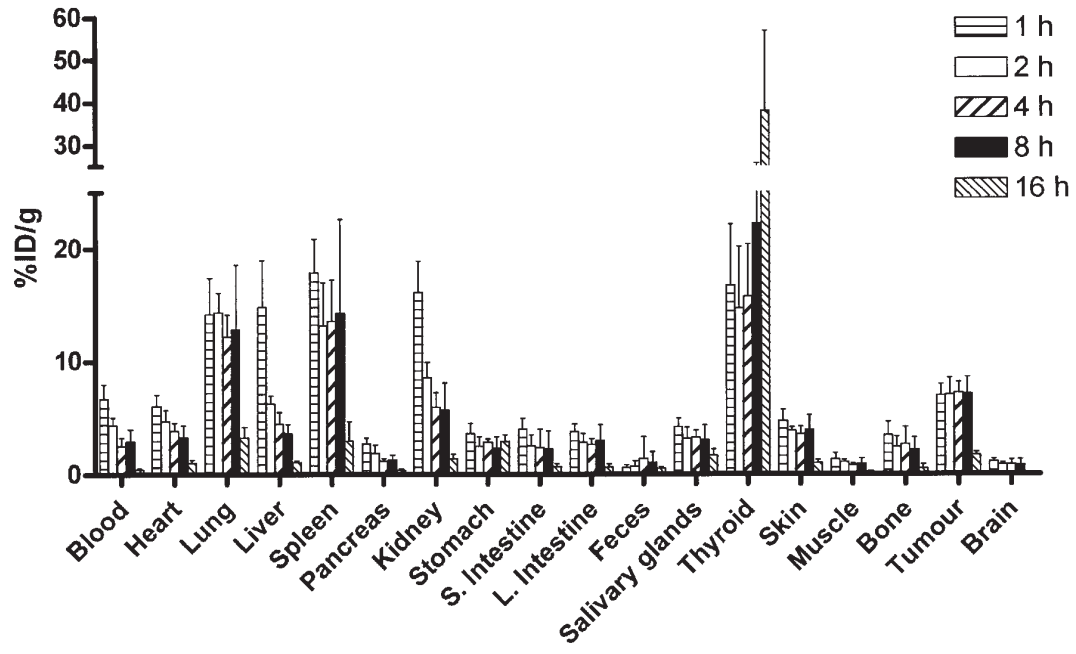

Figure 6. Biodistribution of [^{211}At]PAB-$Z_{HER2:342}$-cys after co-administration of L-lysine and Na-thiocyanate in tumor-bearing nude mice. Values are the mean from four mice. Error bars are standard deviations. The thyroid uptake was calculated using a standard thyroid weight (5 mg for a 20 g mouse). The inserted plot shows the specificity of the tumor uptake, where the blocked data represent the tumor uptake after co-administration of unlabeled $Z_{HER2:342}$-cys to block specific sites. The box extends from the 25th percentile to the 75th percentile with a line at the median. The bars show the highest and lowest value.

Table I. Calculation of absorbed dose in different organs and tissues after exposure to [^{211}At]PAB-$Z_{HER2:342}$-cys after co-administration of L-lysine and Na-thiocyanate.

	Absorbed dose (Gy/MBq)	Standard deviation (Gy/MBq)
Blood	1.39	0.13
Heart	1.18	0.15
Lung	3.78	0.71
Liver	1.66	0.18
Spleen	4.09	1.03
Pancreas	0.45	0.07
Kidney	2.18	0.37
Stomach	1.20	1.59
S. Intestine	0.75	0.22
L. Intestine	0.85	0.16
Salivary glands	1.04	0.15
Thyroid	17.24	51.38
Skin	1.13	0.14
Muscle	0.28	0.07
Bone	0.72	0.16
Tumor	2.05	0.19
Brain	0.25	0.06

For comparison, in the ^{125}I case, ~2/3 of the tumor uptake could be removed after blocking the specific uptake (1). However, the fact that some of the ^{211}At uptake could be displaced (Fig. 3) indicate at least some HER-2-specific tumor uptake of ^{211}At.

In a first approach to overcome this problem, a decaborate-based linker molecule was tested. It has been suggested that the release of free ^{211}At *in vivo* is a result of the C-At bond being weaker than the C-I bond, and that the problem might be solved using decaborate-based linker molecules instead of the benzamide derivates most often used, since the B-At bond is stronger than the C-At bond (19). This hypothesis is strengthened by our study with [^{211}At]B10-$Z_{HER2:342}$-cys. The high levels of radioactivity in lungs, stomach, thyroid and salivary glands were drastically reduced when the decaborate-based linker was used. However, a new problem was encountered, high uptake in the liver and kidneys, probably as a result of the residualizing properties of the decaborate-based linker.

The next approach was to go back to the PAB linker and evaluate methods to reduce the *in vivo* degradation and uptake of free ^{211}At. As seen in the biodistribution of [^{125}I]PIB-$(Z_{HER2:4})_2$ (Fig. 2) (1), the highest concentration of radioactivity was found in the kidneys. It is thus reasonable to assume that kidneys are a site of degradation. The radioactivity concentration in kidney can be reduced by blocking the re-absorption in proximal tubule by administration of L-lysine (20), and hopefully, this approach would result in a decrease in release of free ^{211}At. We also tested if the uptake of free ^{211}At in normal tissues could be blocked by administration of sodium thiocyanate, as was done by Larsen *et al* (21). We found that both L-lysine and Na-thiocyanate significantly reduced the uptake of ^{211}At in some normal tissues, and their combination was most efficient. The kidney uptake was, at the investigated time-point, not affected by L-lysine, but since there was a clear effect of L-lysine in stomach and thyroid, it is likely that the effect on the kidney was no longer detectable at the 4-h time-point.

To determine if the second approach was good enough for testing in a therapeutic setting in mice, a full biodistribution in tumor-bearing mice was performed. Multiple time-points were analyzed, enabling estimation of absorbed dose for all organs. The effects of the L-lysine and Na-thiocyanate in this animal model were similar to those found in the normal mouse model, with a reduced uptake in stomach, salivary glands and thyroid. However, the concentrations in liver and spleen were higher at all time-points when L-lysine and Na-thiocyanate was administered. This was not observed in the results shown in Fig. 5, and might be due to the fact that different affibody molecules were used. Surprisingly, the kidney concentrations were unaffected by the L-lysine at all time-points. Thus, the effects of the L-lysine administration cannot be explained by a decrease in kidney uptake of the radiolabeled compound, resulting in decreased degradation of the compound in the kidneys and release of free radiolabeling into the system, as previously discussed. The lack of effect of L-lysine on renal uptake of radiolabeling has been observed previously (22) and can possibly be explained by the already low kidney levels.

The dosimetry calculation showed that the thyroid received the highest radiation dose from ^{211}At, ~8 times more than the tumor. Also the lungs and spleen received a higher dose than the tumor, about twice that of the tumor. Liver and kidneys were exposed to about the same dose as the tumor. The lung is assumed to be a critical organ, making it imperative that the dose to the lungs must be further decreased before this approach can be applied in a therapeutic setting.

In conclusion, changing from one radiohalogen to another (i.e. from ^{125}I to ^{211}At), and/or changing linker molecule in the radiolabeling process, can result in dramatic changes in the biodistribution when small targeting agents, like affibody molecules, are used. The best solution found so far, when applying ^{211}At labeled affibody molecules for therapy, seems to be to use the PAB linker and to administer the conjugate in combination with L-lysine and Na-thiocyanate. However, the remaining problem with high concentrations of the radionuclide in e.g. lungs and spleen limits the use for this setting in radionuclide therapy. We believe that the high stability indicated when the decaborate-based linker molecules were used is essential for successful therapy, and further optimization in that field is now planned.

Acknowledgements

We wish to thank Fredrik Nilsson at Affibody AB for providing the affibody molecules used in this study and Veronika Asplund Eriksson for assistance with the cells. We thank Holger Jensen at the PET and cyclotron unit at Rigshospitalet in Copenhagen, Denmark, for production of the ^{211}At. The study was financially supported by the Swedish Cancer Society [Grant no. 0980-B04-17XCC (040171)]. The animal experiments were performed with permission from the local animal research committee. Preparation of the decaborate-based labeling molecule was funded by NIH (5 RO1 CA113431). We thank Quanta BioDesign (Powell, OH) for the kind donation of the NHS-3-Maleimido-propionate.

References

1. Mattes MJ: Radionuclide-antibody conjugates for single-cell cytotoxicity. Cancer 94: 1215-1223, 2002.
2. Tolmachev V, Carlsson J and Lundqvist H: A limiting factor for the progress of radionuclide-based cancer diagnostics and therapy - availability of suitable radionuclides. Acta Oncol 43: 264-275, 2004.
3. Wikman M, Steffen AC, Gunneriusson E, *et al*: Selection and characterization of HER2/neu-binding affibody ligands. Protein Eng Des Sel 17: 455-462, 2004.
4. Steffen AC, Wikman M, Tolmachev V, *et al*: *In vitro* characterization of a bivalent anti-HER-2 affibody with potential for radionuclide-based diagnostics. Cancer Biother Radiopharm 20: 239-248, 2005.
5. Natali PG, Nicotra MR, Bigotti A, *et al*: Expression of the p185 encoded by HER2 oncogene in normal and transformed human tissues. Int J Cancer 45: 457-461, 1990.
6. Press MF, Cordon-Cardo C and Slamon DJ: Expression of the HER-2/neu proto-oncogene in normal human adult and fetal tissues. Oncogene 5: 953-962, 1990.
7. Steffen AC, Orlova A, Wikman M, *et al*: Affibody-mediated tumour targeting of HER-2 expressing xenografts in mice. Eur J Nucl Med Mol Imaging 33: 239-248, 2006.
8. Orlova A, Magnusson M, Eriksson T, *et al*: Tumor imaging using a picomolar affinity HER2 binding Affibody molecule. Cancer Res 66: 4339-4348, 2006.
9. Ekerljung L, Steffen AC, Carlsson J and Lennartsson J: Effects of HER2-binding affibody molecules on intracellular signaling pathways. Tumour Biol 27: 201-210, 2006.
10. Shelly K, Knobler CB and Hawthorne MF: Synthesis of mono-substituted derivatives of closo-decahydrodecaborate(2-). X-ray crystal structures of [closo-2-B10H9CO]- and [closo-2-B10H9NCO]2-. Inorganic Chem 31: 2889-2892, 1992.
11. Persson MI, Gedda L, Jensen HJ, Lundqvist H, Malmstrom PU and Tolmachev V: Astatinated trastuzumab, a putative agent for radionuclide immunotherapy of ErbB2-expressing tumours. Oncol Rep 15: 673-680, 2006.
12. Koziorowski J, Henssen C and Weinreich R: A new convenient route to radioiodinated N-succinimidyl 3- and 4-iodobenzoate, two reagents for radioiodination of proteins. Appl Radiat Isotopes 49: 955, 1998.
13. Zalutsky MR and Vaidyanathan G: Astatine-211-labeled radiotherapeutics: an emerging approach to targeted alpha-particle radiotherapy. Curr Pharm Des 6: 1433-1455, 2000.
14. Vaidyanathan G and Zalutsky MR: Targeted therapy using alpha emitters. Phys Med Biol 41: 1915-1931, 1996.
15. Wilbur DS, Vessella RL, Stray JE, Goffe DK, Blouke KA and Atcher RW: Preparation and evaluation of para-[211At]astatobenzoyl labeled anti-renal cell carcinoma antibody A6H F(ab')2. *In vivo* distribution comparison with para-[125I]iodobenzoyl labeled A6H F(ab')2. Nucl Med Biol 20: 917-927, 1993.
16. Orlova A, Hoglund J, Lubberink M, *et al*: Comparative biodistribution of the radiohalogenated (Br, I and At) antibody A33. Implications for *in vivo* dosimetry. Cancer Biother Radiopharm 17: 385-396, 2002.
17. Garg PK, Harrison CL and Zalutsky MR: Comparative tissue distribution in mice of the alpha-emitter 211At and 131I as labels of a monoclonal antibody and F(ab')2 fragment. Cancer Res 50: 3514-3520, 1990.
18. Hadley SW, Wilbur DS, Gray MA and Atcher RW: Astatine-211 labeling of an antimelanoma antibody and its Fab fragment using N-succinimidyl p-astatobenzoate: comparisons *in vivo* with the p-[125I]iodobenzoyl conjugate. Bioconjug Chem 2: 171-179, 1991.
19. Wilbur DS, Chyan MK, Hamlin DK, *et al*: Reagents for astatination of biomolecules: comparison of the *in vivo* distribution and stability of some radioiodinated/astatinated benzamidyl and nido-carboranyl compounds. Bioconjug Chem 15: 203-223, 2004.
20. Behr TM, Sharkey RM, Juweid ME, *et al*: Reduction of the renal uptake of radiolabeled monoclonal antibody fragments by cationic amino acids and their derivatives. Cancer Res 55: 3825-3834, 1995.
21. Larsen RH, Slade S and Zalutsky MR: Blocking [211At]astatide accumulation in normal tissues: preliminary evaluation of seven potential compounds. Nucl Med Biol 25: 351-357, 1998.
22. Forster GJ, Santos EB, Smith-Jones PM, Zanzonico P and Larson SM: Pretargeted radioimmunotherapy with a single-chain antibody/streptavidin construct and radiolabeled DOTA-biotin: strategies for reduction of the renal dose. J Nucl Med 47: 140-149, 2006.